

Document downloaded from:

<http://hdl.handle.net/10251/55106>

This paper must be cited as:

Puerto García, D.; Griol Barres, A.; Escalante Fernández, JM.; Pennec, Y.; Djafari-Rouhani, B.; Beugnot, J.; Laude, V.... (2012). Honeycomb Photonic Crystal Waveguides in a Suspended Silicon Slab. *IEEE Photonics Technology Letters*. 24(22):2056-2059. doi:10.1109/LPT.2012.2219516.



The final publication is available at

<http://dx.doi.org/10.1109/LPT.2012.2219516>

Copyright Institute of Electrical and Electronics Engineers (IEEE)

Additional Information

“© © 20xx IEEE. Personal use of this material is permitted. Permission from IEEE must be obtained for all other uses, in any current or future media, including reprinting/republishing this material for advertising or promotional purposes, creating new collective works, for resale or redistribution to servers or lists, or reuse of any copyrighted component of this work in other works.”

Honeycomb photonic crystal waveguides in a suspended silicon slab

**Daniel Puerto,¹ Amadeu Griol,¹ Jose M. Escalante,¹ Yan Pennec,²
Bahram Djafari Rouhani,² Jean-Charles Beugnot,³ Vincent Laude,³
and Alejandro Martínez^{1,*}**

*¹Nanophotonics Technology Center, Universitat Politècnica de Valencia, Camino de
Vera s/n, 46022 Valencia, Spain*

*²Institut d'Electronique, Microélectronique et Nanotechnologie, UMR CNRS 8520
Université Lille 1, Villeneuve d'Ascq, France*

³Institut FEMTO-ST, Université de Franche Comté and CNRS, Besançon, France

*Corresponding author: amartinez@ntc.upv.es

Abstract

We report experimental evidence of light guiding at telecom wavelengths along line-defect honeycomb-lattice photonic crystal waveguides created in suspended silicon slabs. Numerical results show that the guided bands correspond to modes below the cladding light line so they are inherently lossless, although the measurements show quite high losses owing to fabrication imperfections. Honeycomb photonic crystals are a suitable platform for confining light and sound in nanoscale waveguides.

Photonic crystal slabs (PCSs) consist of a periodic lattice of holes perforating a high-index semiconductor film so that light confinement in the film is achieved by means of total internal reflection and the periodicity gives rise to bandgaps to forbid guided-light propagation at certain wavelengths. The introduction of line defects in PCSs has become a powerful way to create light waveguides at the nanoscale with some special properties such as lossless sharp bending [1] or slow-light propagation [2]. The triangular lattice has become very popular because it provides a very wide bandgap for even-parity modes (which can be excited using TE polarized light) in PCSs [3]. However, there are other types of lattice that display other features that can be of interest for the creation of PCS-based circuits. Specifically, square- and honeycomb-lattice suspended PCSs have been shown to possess bandgaps not only for photons but also for acoustic waves [4]. If such PCSs are designed to present bandgaps for guided photons at optical communication wavelengths around 1550 nm, bandgaps for phonons appear at frequencies of some gigahertz. It has to be stressed that the simultaneous confinement and enhanced interaction of photons and phonons in periodic nanostructures has become a hot-topic in recent years giving rise to the field known as optomechanics [5,6]. Therefore, it becomes clear that square- and honeycomb-lattice PCSs can become an important platform for optomechanics as well as for demonstration of other interesting acousto-optical effects such as stimulated Brillouin scattering [7] at the nanoscale. In this work, we demonstrate for the first time to the best of our knowledge the guiding of light at telecom wavelengths along photonic waveguides created by introducing line defects in honeycomb-lattice PCSs built on suspended-silicon slabs.

Honeycomb-lattice PCSs can be designed to display a complete photonic bandgap in the sense of forbidding guided modes for both odd and even symmetries [4]. However, this complete bandgap turns to be quite narrow, which could be very limiting for some applications. From this point of view, it would be more useful to have a wider bandgap

for a given symmetry, since in PCS-based devices we can separately excite even or odd modes by properly selecting the polarization of the input light. In other words, a photonic bandgap occurring for a unique symmetry (odd or even) should be enough for most usual functionalities, such as cavities, waveguides or splitters. For instance, a silicon PCS with $h/a = 0.6$ and $r/a = 0.25$ (a is the lattice period, h is the slab thickness and r is the radius of the holes) displays a photonic band gap for odd-parity guided modes in the interval $[0.387, 0.437]$ expressed in normalized frequency units of $\omega a/2\pi c$. If we choose $a=650$ nm, such a PCS would support a photonic bandgap around 1550 nm and an acoustic bandgap around 5 GHz [4]. It is worth mentioning that this PCS could be readily manufacturable using state-of-the-art nanofabrication processes.

A photonic waveguide can be created by introducing a line-defect along the ΓJ direction in the otherwise periodic lattice as schematically depicted in Fig. 1(a). By varying the parameter d , we control the waveguide width and the amount of odd-parity – with respect to the xy -plane that divides the slab into two halves - guided modes appearing in the photonic bandgap as shown in Fig. 1(b). It can be seen that when d is increased there are photonic bands that drop from the continuum of guided modes above the bandgap. The frequency region of such bands that is below the light cone corresponds to truly guided modes which are inherently lossless, in contrast the guided modes in honeycomb-lattices fabricated in semiconductor heterostructures with small-index contrast in the vertical direction [7]. Fig. 1(c) shows the electric and magnetic field patterns of the first guided mode in a waveguide with $d=1.6A$ at the k -point highlighted in Fig. 1(b). Interestingly, the guided bands are quite flat so they will display slow-light propagation, which could give rise to enhanced acousto-optical interactions [9]. For instance, the first guided band shows a group velocity of the order of $c/10$ far in the linear dispersion region (far from the band edge) as depicted in Fig. 1(d). The group velocity can be further reduced down to $\sim c/100$ for the $d=1.4A$ waveguide, although in

this case an efficient excitation of the guided mode would be more difficult owing to a large group-velocity mismatching.

We fabricated honeycomb-lattice PCS waveguides by using a direct writing photolithography process carried out with standard nanofabrication tools. A 170 nm PMMA-950K layer was coated on top of a silicon-on-insulator sample with 390 nm silicon thickness. Then we used electron beam lithography to create the patterns into the resist prior to a standard PMMA developing process. The samples were then etched by using Reactive Ion Etching in an Inductively Coupled Plasma tool. Finally, an AZECI-3027 photo resist mask was created by using ultraviolet lithography in order to release the silicon membrane by using a buffered HF bath. Figure 2 shows scanning electron micrographs images of the released regions in the fabricated sample. The connecting silicon waveguides were widened up to a 3- μm width to facilitate the coupling from external optical fibers (not shown in the images).

Optical characterization was carried out by using an end-fire technique. Light from a tunable laser source (1260 to 1630 nm) was coupled into the sample using a lensed fiber, and the output light was collected by an objective onto a power detector. The measured power was normalized to the response of a 400-nm-width straight photonic waveguide of which 20 μm were suspended and that was built on the same sample. The measured spectra for TM-polarized light are shown in Fig. 3(a) for different values of d . For $d=A$, the waveguide width is zero so we have a perfect honeycomb lattice photonic crystal and a high attenuation (~ 35 dB) in the wavelength region corresponding to the predicted odd bandgap is observed. This high attenuation is also observed when the lattice is arranged so that incidence is along the ΓX direction, which confirms the prediction of a two-dimensional photonic bandgap for odd modes. When d is increased, high transmission zones appear in the region inside the calculated odd-parity photonic bandgap. We partly attribute this high-transmittance to the excitation of

the guided modes calculated before (see Fig. 1(b)). However, we do not observe discrete modes but a continuous band covering almost the full measured wavelength range. This can be due to the excitation of leaky modes above the light line (not shown in Fig. 1(b) for the sake of simplicity) as well as the collection of light directly coming from the lensed fiber. Therefore, to fully observe the excitation of the predicted guided modes, longer waveguides are required so that only truly guided modes can reach the PCS waveguide end. Measurements for longer PCS waveguides with $d=1.6A$ are shown in Fig. 3(b). The interface between the input/output silicon waveguides and the PCS waveguide was as in Fig. 3 regardless of the total length. In Fig. 3(b) it can be seen that when the length is increased, three narrow transmission bands are kept in the bandgap (marked with arrows). We believe that these high transmission regions correspond to the guided modes within the bandgap. It is especially interesting to notice that the two lower bands are trimly distinguished for all the lengths probably because an easier excitation owing to modal symmetry issues. A rough estimation of the propagation losses for the first mode gives us a value of 100 dB/mm. This is a quite high value that can be explained by two main reasons. First, propagation losses are produced mainly by scattering in the etching-induced roughness at the sidewalls, and this scattering grows with the waveguide thickness, so we can expect higher losses in our waveguides than in typical triangular-lattice photonic crystal waveguides created in 220-nm thick silicon. And secondly, we are exciting slow-light modes so the propagation losses will grow with the inverse of the group velocity. We are confident in that by improving the fabrication processes, propagation losses of the order of 10dB/mm are under reach, so these waveguides could be used for coupling light with guided acoustic modes.

Transmission calculations, performed using a 3D-finite-difference time domain code, are presented in Fig. 4 for the perfect PCS and for the waveguide structure with $d=1.6A$ with a length of 14 periods ($\sim 10 \mu\text{m}$). The position of the band gap, highlighted in blue,

is in good agreement with the dispersion curve calculation (Fig. 2(b)). The insertion of the waveguide leads to a transmission inside the band gap. This transmission is formed by four peaks which reduced frequencies correspond to the ones observed in the dispersion curve, which is in a reasonable good agreement with the experimental results (Fig. 3(b)), with the main difference that only three peaks were revealed experimentally. We think that the fourth band can be obscured by not-guided light that is captured by the camera.

Interestingly, we observe in simulations and experiments that for the structure without defect the transmission is quite low even at frequencies over the predicted bandgap for both directions of incidence. This low transmittance can be explained by considering the excitation of multiple photonic modes in the photonic crystal region. In this case, modes with very different wave-vectors (including modes with high transverse wave vectors as a consequence of the high divergence of the light coming from the narrow input silicon waveguide) will be excited and they can also couple slab-modes out of the photonic-crystal region so that an very small amount of power will be finally coupled to the output waveguide. This mechanism also explains why a high transmission is observed above the bandgap region when the line-defects are introduced: the waveguide can be seen as a high-index region between two PCSs that reduced the divergence of the input signal coming from the input waveguide and provides a light channel towards the output waveguide by the mechanism of total-internal reflection as in conventional dielectric waveguides.

In summary, we have demonstrated experimentally light guiding in the 1550 nm wavelength region along line-defects created in suspended silicon photonic crystal with a honeycomb lattice of holes. Our calculations show that the guided modes are below the light line so they are lossless in theory. Since the studied photonic crystal structure also displays a band gap for gigahertz acoustic waves, it can be a proper two-

dimensional platform for simultaneous guiding and enhanced interaction of light and sound as well as to observe novel acousto-optical and optomechanical effects.

This research has received funding from the EC Seventh Framework Programme (FP7/2007-2013) under grant agreement number 233883 (TAILPHOX).

References

1. A. Mekis, J. C. Chen, I. Kurland, S. Fan, P. R. Villeneuve, and J. D. Joannopoulos, *Phys. Rev. Lett.* 77, 3787-3790 (1996)
2. M. Notomi, K. Yamada, A. Shinya, J. Takahashi, C. Takahashi, and I. Yokohama, *Phys. Rev. Lett.* 87, 253902 (2001).
3. J. Joannopoulos and J. Winn, *Photonic Crystals: Molding the Flow of Light* (Princeton Univ. Press, 2008).
4. Y. Pennec, B. Djafari Rouhani, E. H. El Boudouti, C. Li, Y. El Hassouani, J. O. Vasseur, N. Papanikolaou, S. Benchabane, V. Laude, and A. Martinez, *Opt. Express* 18, 14301-14310 (2010).
5. M. Eichenfield, R. Camacho, J. Chan, K. J. Vahala, and O. Painter, *Nature* 459 (7246), 550–556 (2009).
6. M. Eichenfield, J. Chan, R. Camacho, K. J. Vahala, and O. Painter, *Nature* 462 (7269), 78–82 (2009).
7. P. T. Rakich, C. Reinke, R. Camacho, P. Davids, and Z. Wang, *Phys. Rev. X* 2, 011008 (2012).
8. P. Ma, P. Kaspar, Y. Fedoryshyn, P. Strasser, and H. Jäckel, *Opt. Lett.* 34, 1558-1560 (2009).
9. V. Laude, J.-C. Beugnot, S. Benchabane, Y. Pennec, B. Djafari-Rouhani, N. Papanikolaou, J. M. Escalante, and A. Martinez, *Opt. Express* 19, 9690-9698 (2011).

Figure captions

Figure 1. (a) Scheme of the proposed waveguides controlled by the parameter d ($d=A$ means a perfect structure without waveguide). (b) Calculated bands for different values of d : A (black curves), $1.2A$ (red curves), $1.4A$ (green curves) and $1.6A$ (blue curves). (c) Snapshots of electric and magnetic fields and (d) calculated group velocity of the first guided mode for $d=1.6A$. Parameters: $h/a = 0.6$, $r/a = 0.25$, $n_{Si}=3.45$.

Figure 2. Scanning electron microscopy images of the fabricated waveguides along ΓJ : (a) $d=A$ (no waveguide), (b) $d=1.2A$ (c) $d=1.4A$ (d) $d=1.6A$.

Figure 3. Measured normalized spectra for TM-polarized light and for different values of d and PCS waveguide lengths. (a) $d=A$ (black), $d=1.2A$ (red), $d=1.4A$ (green), $d=1.6A$ (blue). The grey curve corresponds to a perfect crystal but with incidence along the ΓX direction. The total length of the PCS region (with or without waveguide) is $10 \mu\text{m}$; (b) Waveguides with $d=1.6A$ and total length of $10 \mu\text{m}$ (red), $30 \mu\text{m}$ (green), $50 \mu\text{m}$ (blue), $100 \mu\text{m}$ (brown), $150 \mu\text{m}$ (orange), and $200 \mu\text{m}$ (violet). The arrows highlight the observed transmission peaks in the $50 \mu\text{m}$ waveguide response..

Figure 4. Normalized transmission calculations using a 3D-finite-difference time domain code for a perfect PCS and for the waveguide with $d=1.6A$ and a length of 14 periods ($\sim 10 \mu\text{m}$).

Figures

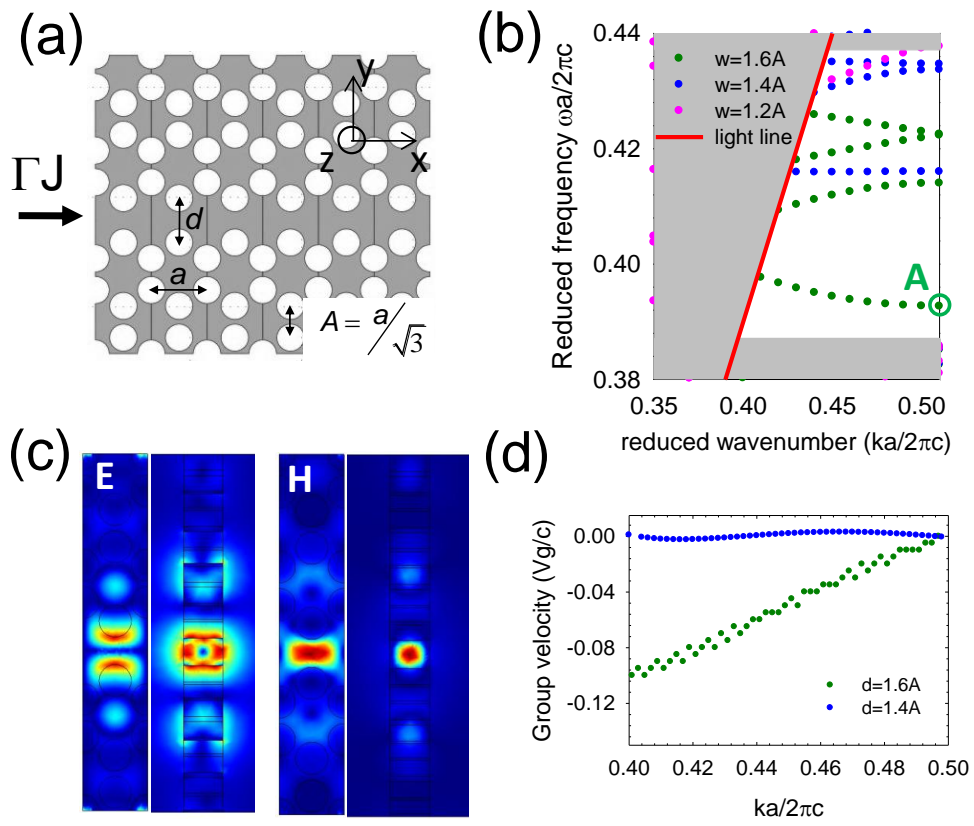


Figure 1

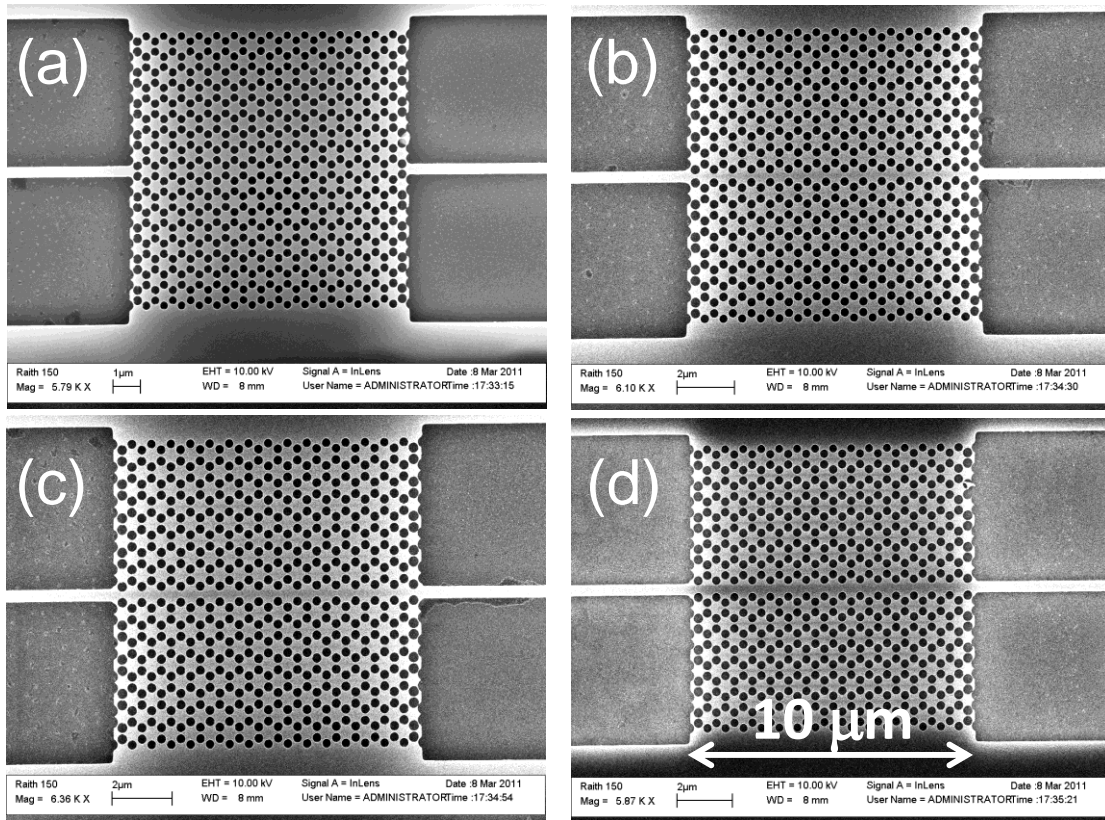


Figure 2

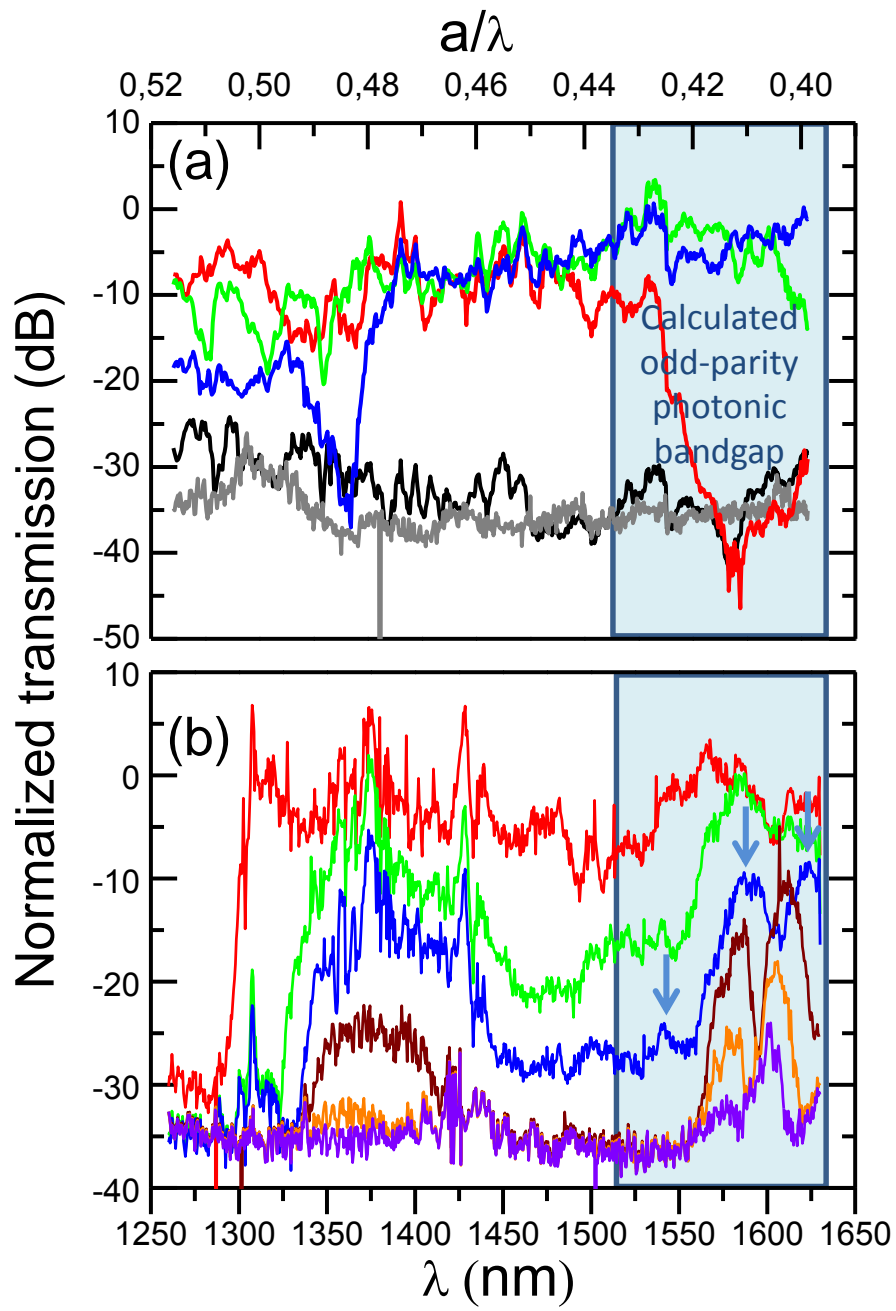


Figure 3

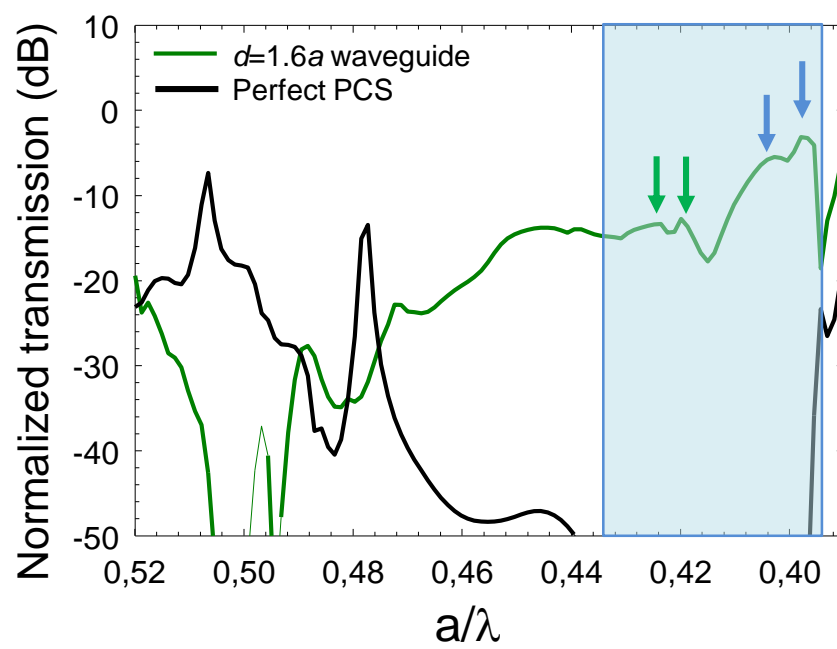


Figure 4